Available online at www.sciencedirect.com
ScienceDirect
Journal of Membrane Science 310 (2008) 418–430
journal of MEMBRANE SCIENCE
www.elsevier.com/locate/memsci

Reducing power losses caused by ionic shortcut currents in reverse electrodialysis stacks by a validated model

J. Veerman [a], J.W. Post [a,c], M. Saakes [a], S.J. Metz [a,*], G.J. Harmsen [b]

[a] *Wetsus, P.O. Box 1113, 8900 CC Leeuwarden, The Netherlands*
[b] *University of Groningen, Nijenborg 4, 9747 AG Groningen, The Netherlands*
[c] *Sub-department of Environmental Technology, Wageningen University, P.O. Box 8129, 6700EV Wageningen, The Netherlands*

Received 27 July 2007; received in revised form 6 November 2007; accepted 11 November 2007

Abstract

Both in electrodialysis and in reverse electrodialysis ionic shortcut currents through feed and drain channels cause a considerable loss in efficiency. Model calculations based on an equivalent electric system of a reverse electrodialysis stack reveal that the effect of these salt bridges could be reduced via a proper stack design. The critical parameters which are to be optimized are ρ/r and R/r, where ρ is the lateral resistance along the spacers, R is the resistance of the feed and drain channels between two adjacent cells, and r is the internal resistance of a cell. Because these two parameters are dimensionless, different stacks can be easily compared. The model is validated with two experimental stacks differing in membrane type and spacer thickness, one with large ionic shortcut currents and one where this effect is less. The loss in efficiency decreased from 25 to 5% for a well-designed stack. The loss of efficiency in reverse electrodialysis and in electrodialysis can be reduced with the aid of the design parameters presented in this paper.

Keywords: Reverse electrodialysis; Electrodialysis; Modeling; Ionic shortcut currents; Parasitic currents; Current leakage; Stack design; Optimization

1. Introduction

Reverse electrodialysis (RED) is one of the possible processes for generating energy from the salt gradient between river and sea water [1]. Already in 1953 Pattle showed the possibility of this method [2]. A typical RED stack consists of a variable number of alternating cation and anion exchange membranes. The compartments between the membranes are fed in turn with a concentrated and a diluted salt solution, for instance of sea and river water. In Fig. 1 the situation is drawn for a stack with four cells.

Parasitic currents, also called current leakage, cause a loss in performance in both electrodialysis (ED) and reverse electrodialysis. There are two sources of these parasitic currents. Firstly, in an ion exchange membrane, besides the wanted transport of the counter-ions, there is a transport of co-ions due to the fact that membranes are not 100% selective. Secondly, there are ionic shortcut currents, arising from the transport of ions through the feed and drain channels. These channels act as salt bridges between the compartments. Transport of ions through these salt bridges occurs due to an electrochemical potential difference between adjacent cells. Both types of parasitic currents cause in a RED stack a reduction of power and a decrease in fuel efficiency in a RED stack. Reduction of the co-ion transport is a matter of membrane optimization and is left out of consideration in this paper. However, the effect of the ionic shortcut currents is strongly related to the stack design and is discussed here.

That ionic shortcut can cause efficiency loss in electrodialysis was understood already in an early stage of the development of ED. Mandersloot and Hicks made already in 1966 a mathematical model of an ED stack and concluded that it is important to have a low channel conductivity between the compartments [3]. The efficiency loss is more drastic if the salt concentration becomes higher. Some measures to restrict the ionic shortcut currents are suggested:

(i) In Japan already in the sixties all edible salt was produced from seawater with electrodialysis. The high salt concentrations used in this process cause severe ionic shortcut

* Corresponding author. Tel.: +31 58 284 6200.
E-mail address: sybrand.metz@wetsus.nl (S.J. Metz).

0376-7388/$ – see front matter © 2007 Elsevier B.V. All rights reserved.
doi:10.1016/j.memsci.2007.11.032

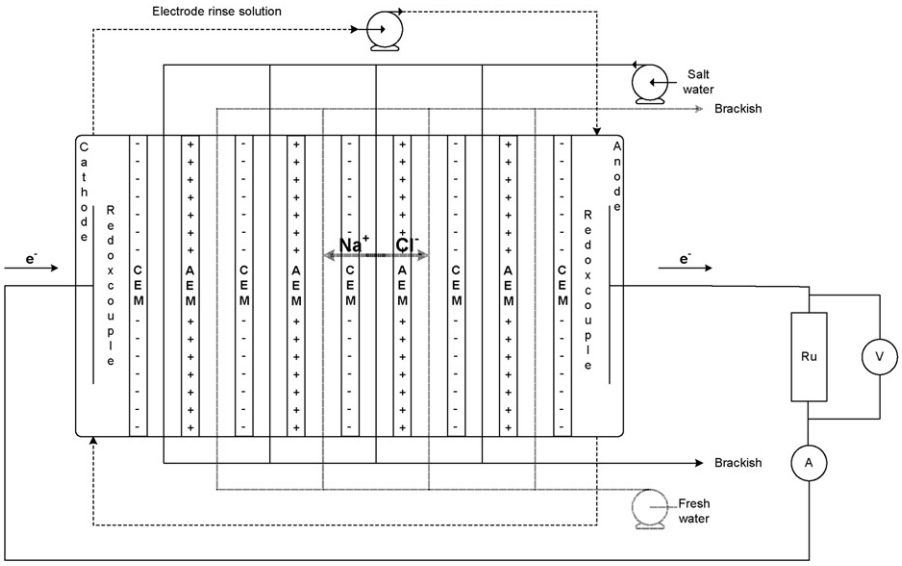

Fig. 1. Schematic representation of a reverse electrodialysis stack with four cells.

losses in the system. Yamane et al. have found that the use of separate unit cells in the production of brine from sea water can reduce the ionic shortcut current by more than 30% [4]. The individual cells have separate feed tubes. The long conductive paths through these tubes give enough resistance to reduce the parasitic currents effectively.

(ii) Air bubbles can be added to the feed. This decreases the ionic shortcut currents and has less effect on the water transport in the stack.

(iii) Rotating valves which act as barriers to the electrolytic currents [5].

(iv) An alternative method is the serial feed. The sea water is directed successively through all sea water compartments of the stack. These compartments are connected alternating at the top and at the bottom, causing a zigzag flow. The same holds for the river water. In this case a possible ionic shortcut current should pass a much longer pathway and is therefore significantly reduced. However, this causes also a much higher fluid resistance. However, a combination of parallel and serial feed can be realistic for an optimal design.

(v) The use of spiral wound modules makes the feed and drain channels superfluous. In fact there are only two compartments: the diluate and the concentrate [6–8].

Especially for bipolar cell stacks, the electrical leakage has been studied by different groups. In 1979 Kuhn and Booth

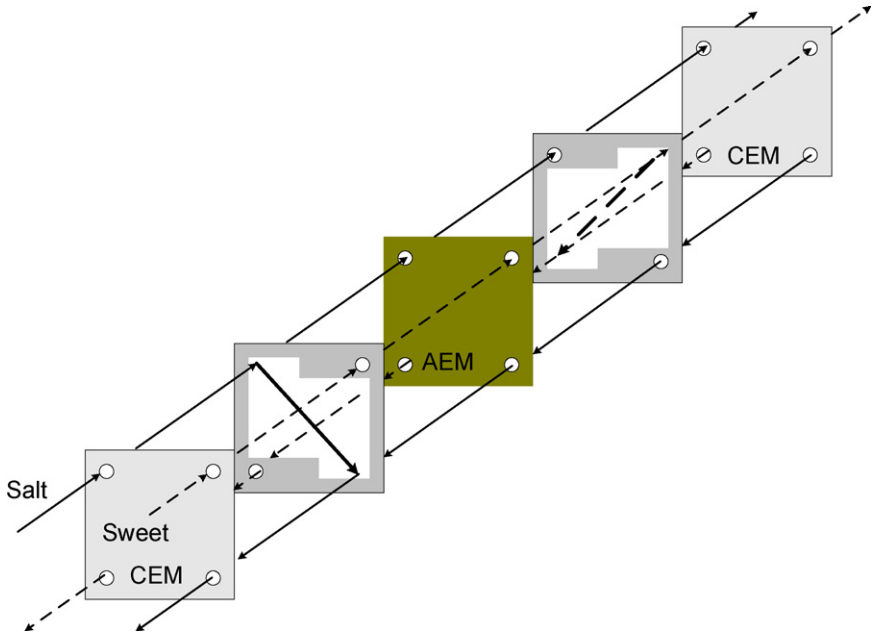

Fig. 2. Fluid transport through the feed and drain channels of a reverse electrodialysis stack. The solid lines represent the salt water flow and the dashed lines the sweet water flow. The membranes (CEM and AEM) are separated by the gaskets.

reviewed the state-of-art in that field [9] and calculated the ionic shortcut currents as function of the place in a bipolar cell stack. Pretz and Staude [10] used a RED system with bipolar membranes and observed a limiting value of the open circuit voltage (OCV) with the increase of the number of membranes. Rubinstein et al. [11] explained this effect by ionic shortcut currents.

The objective of this work is to quantify the efficiency losses due to ionic shortcut currents in (reverse) electrodialysis. These effects can be modeled via an equivalent electrical circuit and are validated experimentally. Experiments are performed with two different stack designs, one with a large ionic shortcut current and another where this effect is less. The model is calibrated by experiments with small stacks (1, 2, ..., 5 cells) and validated by experiment with large stacks (10, 20, ..., 50 cells). Model and experiments are in good agreement and this shows the possibility of managing the ionic shortcut currents within acceptable proportions.

2. Theory

2.1. Reverse electrodialysis

A RED stack with four cells is drawn in Fig. 1. Each cell contains a cation exchange membrane (CEM), a compartment with a concentrated salt solution, an anion exchange membrane (AEM), and a compartment with a lower salt concentration. The last cell is closed with an extra cation exchange membrane. The 'fuel' consists of a concentrated and a diluted salt solution, for instance sea and river water.

The Na^+ ions from the sea water tend to diffuse through the cation exchange membranes and cause a positive potential on the left side of the stack. In the same way, the Cl^- ions diffuse through the anion exchange membrane in the reverse direction, also resulting in a positive potential on the left side of the stack. Transport of ions through the membranes occurs if an electrical load is connected to the electrodes. Externally there is a normal electrical current but in the cell this is an ionic current. The ionic current in the cells is converted to an electron current at the electrodes by redox reactions.

These redox reactions can be facilitated by means of a solution of $K_4Fe(CN)_6$ and $K_3Fe(CN)_6$ (potassium iron(II) hexacyanoferrate and potassium iron(III) hexacyanoferrate) in a bulk of NaCl in combination of inert electrodes. The iron(III) complex is reduced on the cathode and the iron(II) complex is reoxidized on the anode. Because the electrode rinse is recirculated through both electrode compartments, the original Fe(III)/Fe(II) ratio is maintained and there is no net chemical reaction.

$$Fe(CN)_6{}^{3-} + e \rightleftarrows Fe(CN)_6{}^{4-}, \quad E_0 = 0.36\,V$$

2.2. The electromotive force

The theory about reverse electrodialysis was formulated by Weinstein and Leitz [12], Clampitt and Kiviat [13], Jagur-Grodzinski and Kramer [14] and Lacy [15]. The potential to the left off a given cation exchange membrane in Fig. 1, generated by the diffusion of Na^+ ions, is given by:

$$E = \alpha_{CEM}\frac{RT}{zF}\ln\left(\frac{a_c^+}{a_d^+}\right) \quad (1)$$

where E is the generated electromotive force (EMF), α_{CEM} the permselectivity of the cation exchange membrane, z the valency ($z = 1$ for Na^+), R the gas constant, F the Faraday constant and a_c^+ and a_d^+ the activities of the sodium ion in the concentrated and diluted compartments. This formula holds also for the potential caused by the diffusion of Cl^- ions through an anion exchange membrane if α_{AEM} is taken for the permselectivity and a_c^- and a_d^- for the activity of the Cl^- ion. Activities can be calculated with the extended Debye-Hückel formula [16]. With formula 1, the voltages across a 100% selective membrane can be calculated. For pure NaCl solutions of 1 and 30 g/L this gives values of 0.080 V for a CEM and 0.078 V for an AEM, or together 0.158 V for a cell.

2.3. Ionic shortcut currents

A proper RED stack has a high power output characterized by the specific power (P_{spec}), which is the power generated at one square meter of membrane. An equally important process parameter is the fuel efficiency: the amount of obtained energy in relation to the theoretical maximum for a given amount of fuel.

As explained in the introduction, there are two kinds of parasitic currents: firstly co-ion transport through the membranes due a restricted selectivity and secondly ionic shortcut currents, arising from the transport of ions through the feed and drain channels (Fig. 2). Both types of parasitic currents cause a loss of power as well as a reduction of the fuel efficiency in a RED stack.

Three ionic shortcut currents can be identified in a RED stack: (i) in the electrode rinse solution. The anode compartment is connected with the cathode compartment by the electrode rinse loop as shown in Fig. 1. This shortcut current is easily prevented by choosing an appropriate length of the tubing causing a higher resistance. (ii) Between the river water compartments. This shortcut current has been neglected because the salt concentration is too low to cause a significant shortcut current. (iii) Between the seawater compartments. These latter shortcut currents are shown in Fig. 3. Reducing these shortcut currents is the subject of this paper.

In Section 2.4 the theory of the power production in small stacks is formulated. In these stacks shortcut currents are not significant because the resistance of the bypass circuit is relatively high. The model is simple and the calculation of the power production can be done easily. In Section 2.5 a model is introduced involving the shortcut currents in the salt water system. This model should be used if the stack has a large number of cells, but can be applied also to small and to very large stacks. In Section 2.6 the model is simplified for very large stacks resulting in a simple equation for the relative power (Eq. (13)).

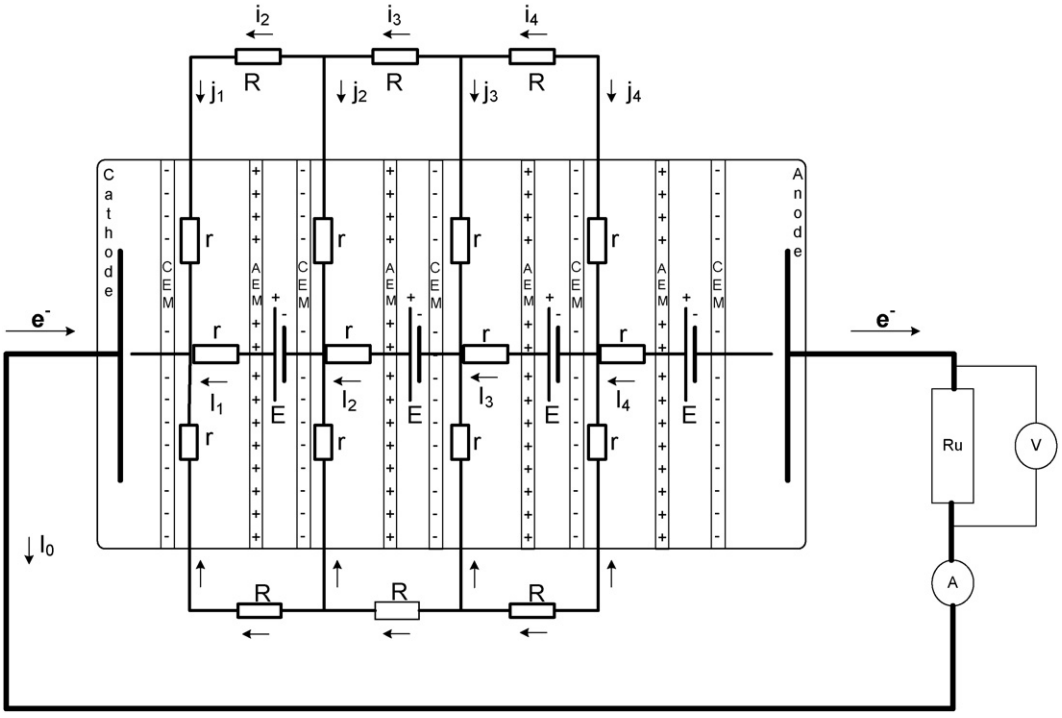

Fig. 3. Ionic currents. The currents designated with i_n ($n = 2, 3, 4$) and j_n, ($n = 1, \ldots, 4$) are unwanted shortcuts. All given currents are positive except j_3 and j_4 which are negative.

2.4. Internal resistance and power production of small stacks

In ideal stacks there are no ionic shortcut currents. In practice, these stacks consist of only a few cells. Stacks with a maximum of 5 cells are considered as ideal in this paper. The internal resistance R_i of an ideal stack depends on the cell resistance r, the number of cells N and the resistance of the electrode system R_{el}.

$$R_i = Nr + R_{el} \tag{2}$$

In the electrode resistance R_{el} is also included the resistance of one of the outer membranes (the other outer membrane is formally part of one of the cells).

The cell resistance r is the sum of the resistances of two membranes (R_{AEM} and R_{CEM}) and two water compartments (R_{river} and R_{sea}).

$$r = R_{AEM} + R_{CEM} + R_{river} + R_{sea} \tag{3}$$

If there is no spacer in the water compartment, the resistance of the water compartments, R_{comp} can be calculated from the specific conductivity σ (S/m) of the salt solution, the area A_{cell} (m^2) and the thickness δ (m) of the compartment. A correction is used for the volume occupied by the spacer material. The void factor f_v expresses the relative volume available for the salt solution (void volume).

$$R_{comp} = \frac{1}{f_v}\frac{1}{\sigma}\frac{\delta}{A_{cell}} \tag{4}$$

An ideal RED installation without complicating shortcut currents, behaves like a normal battery and its current I is given by:

$$I = \frac{E}{R_i + R_u} \tag{5}$$

where E is the electromotive force, R_i the internal resistance of the stack and R_u the external load resistance.

The power dissipated in the external resistance R_u in this ideal system is:

$$P_u = I^2 R_u = \left(\frac{E}{R_i + R_u}\right)^2 R_u \tag{6}$$

From Eq. (6) it follows that a maximum of P_u arises if $R_u = R_i$. In this case the terminal voltage is $V_t = (1/2)E$. The efficiency (Eff) is the fraction of the power delivered to R_u and the total power dissipation in R_i and R_u.

$$\text{Eff} = \frac{I^2 R_u}{I^2 R_i + I^2 R_u} = \frac{R_u}{R_i + R_u} \tag{7}$$

At the condition for maximal power ($R_u = R_i$) even in an ideal system the efficiency is no higher than 50%. A higher efficiency can by achieved (by taking $R_u > R_i$) at the expense of a decreased power output.

2.5. Modelling the stack

An equivalent system, a model for a real stack with four cells and all shortcut circuits caused by the concentrate feed, is given in Fig. 4. This stack is connected to an external load. The

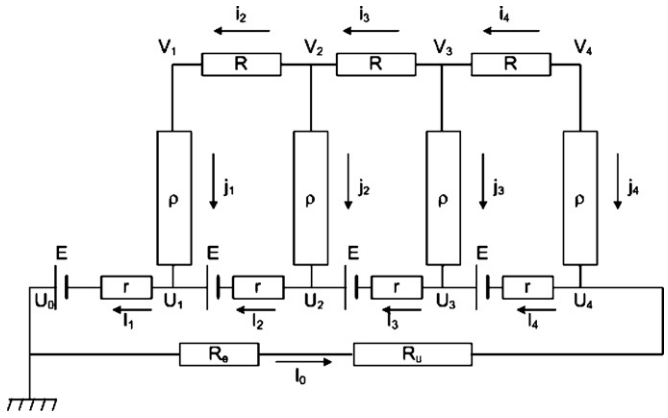

Fig. 4. Equivalent circuit model for a RED stack with 4 cells. r is the internal resistance of a cell, ρ the resistance across a salt water space, R the resistance in the feed and drain channels between two salt water compartments, R_e the resistance of the electrode system, R_u the external load, I is the current through the membrane, i the current through the feed and drain channels, j the lateral current leakage along the membrane surface, U the potential at the centre of the membrane, V the potential in the feed and drain channel, and E the electromotive force of one cell.

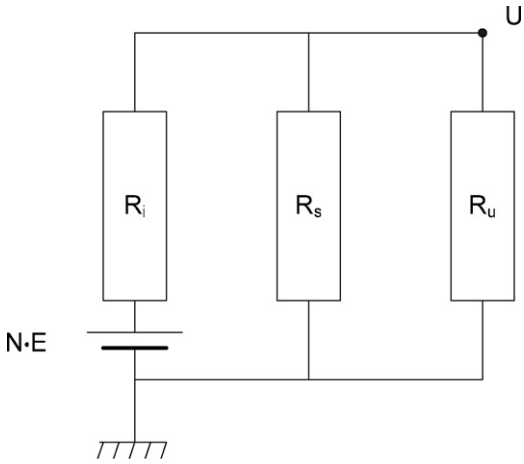

Fig. 5. Simplified equivalent circuit model for a very large stack. The stack EMF is N times the cell EMF. R_i is resistance of the N cells, R_s the feed and drain channel resistance and R_u the external load. Because the stack is very large, the number of lateral spacer resistances connected parallel is so large that these can be omitted from the model.

nomenclature of the symbols follows the model of Rubinstein et al. [11]. The directions of the currents are arbitrarily designated. The resistors ρ are the lateral resistances along the spacers, from the middle to the drain and the feed. The resistors R are the resistances of the feed and drain channels through the stack and r is the internal resistance of a cell. For simplicity, only the shortcut by the sea water is taken into account. Shortcut by the river water is ignored because the conductivity in this part is much lower.

In fact, the equivalent circuit model in Fig. 4 is a summary of the circuit drawn in Fig. 3. For reasons of symmetry, this model is simplified by omitting the lower part from Fig. 3.

Rubinstein et al. [11] have given an approach for solving a system like this in a sophisticated way. However, their model did not include an external load and only the open circuit voltage (OCV) could be calculated.

But adding a load to the system the method of Rubinstein is not applicable and a different method is necessary. This model involves many unknowns: each cell in the stack involves three currents (I, i and j) and two potentials (U and V). The five equations for solving these unknowns are three times the Law of Ohm (over r, over R and over ρ) and two times the law of Kirchhoff (in the junctions U and V). In Mathcad these equations are solved numerically.

2.6. An approximation for very large stacks

There are good ion conducting paths: first the main route through the cell (resistances r) and next the bypass through the feed and drain channel (resistances R). The connection between both paths consists of the lateral spacer resistances (ρ) with a relative high resistance. However, a circuitry of many of such parallel connections result in a relatively low substitution resistance, well enough (in relation to the channel resistance) to realize an ionic shortcut current intruding into the feed and drain channels.

In this case the greater part of the resistance of the ionic shortcut current is formed by the resistances of the feed and drain channels and the lateral spacer resistance can be ignored. In Fig. 5, the model with this approximation is drawn. The EMF of the source, the internal resistance of the stack (R_i) and the total bypass resistance (R_s) can be calculated from the cell parameters (E, r, R) and the number of cells (N): EMF = $N{\cdot}E$, $R_i = N{\cdot}r$ and $R_s = N{\cdot}R$. This little network, easily accessible for a straightforward calculation, gives the next results:

The maximum external power is achieved if the resistance of the load (R_u) equals the internal resistance of the parallel resistances R_i and R_s

$$R_u = \frac{R_i R_s}{R_i + R_s} \tag{8}$$

Fig. 5 shows a very large stack with N cells. The internal resistance is R_i, the shunt resistance (from the shortcut circuit) is R_s and the load (the external resistance) is R_u. We can apply the voltage divider rule to calculate the voltage on point U relative to the ground:

$$U = \frac{R_s || R_u}{R_i + R_s || R_u} N \cdot E \tag{9}$$

The sign || means adding two parallel resistances:

$$R_s || R_u \equiv \frac{R_s R_u}{R_s + R_u}$$

From this the generated power in R_u can be stated:

$$P_u = \frac{U^2}{R_u} = \left[\frac{R_s || R_u}{R_i + R_s || R_u} N \cdot E\right]^2 \frac{1}{R_u} \tag{10}$$

To generate maximum power in R_u, the external load R_u should be equal to substitution value of the internal load and

the shunt resistance:

$$R_u = R_i || R_s$$

Substituting this value for R_u in the foregoing equation leads to

$$P_{max} = \frac{R_s}{4R_i(R_i + R_s)} N^2 E^2 \quad (11)$$

In an ideal stack, the bypass resistance is infinite, resulting in a maximum external power P_{ideal}

$$P_{ideal} = \frac{1}{4R_i} N^2 E^2 \quad (12)$$

The power can also be expressed in relation to this value of P_{ideal}: the power ratio (P_R). The method has been tested on all 75 combinations, mentioned in Section 4.4. It follows that this approximation is suitable if satisfied to the condition $N{\cdot}R/\rho > 1$. In this case the approximation gives a maximal deviation of 10% downward.

$$P_R = \frac{P}{P_{ideal}} = \frac{R}{R + r} \quad \text{if} \quad \frac{N \cdot R}{\rho} > 1 \quad (13)$$

From the experiments, it appeared that the criterion $N{\cdot}R/\rho > 1$ is satisfied at $N = 50$ for poor stacks and at $N = 1000$ or more for well-designed stacks.

2.7. Validation of the model for salinity power production

The optimization with respect to shortcut currents also holds for a salinity power production when the concentrated solution is depleted with ions and the diluted solution is enriched with ions. This causes a decrease of the shortcut currents in the concentrated compartments and an increase in the diluted compartments. If the conductivity of the salt solutions changes linearly with concentration, the net loss due to shortcut currents is equal to net loss that is the case when there is no transport of ions. Moreover, during mixing the internal resistance (r) also decreases, causing increased ratio of R/r and ρ/r and a reduced power loss via shortcut currents. Therefore, optimization of the cell with respect to ionic shortcut currents also holds when ions are transported and salt concentrations are changing.

3. Experimental

3.1. Stack configuration

3.1.1. Stacks

The functional dimensions of the membranes in both types were 10 cm × 10 cm. On the outsides of the stacks cation exchange membranes prevent the transportation of negatively charged iron complexes. Two types of stacks were used both with a variable number of cells. First stacks with Ralex anion and cation exchange membranes (MEGA a.s. Czech Republic) with a thickness of 0.65 mm. The stacks were equipped with regular nonwoven spacers of 1 mm. The radius of the holes in the membranes for the water supply and drain are 5 mm. These stacks are denoted R1.0 in this paper.

Next stacks were used with Fumasep anion and cation exchange membranes FAD and FKD with a thickness of 0.082 mm (Fumatech, Germany). The stacks were provided with polyamide woven spacers with a thickness of 200 μm (Nitex 03–300/51, Sefar, The Netherlands). The radius of the supply holes in the membranes are 4 mm in this case. The stacks of this type are designated as F0.2.

3.1.2. Electrode system

The electrode compartment consisted of a solution of NaCl (1 mol/L) with $K_4Fe(CN)_6$ (0.05 mol/L) and $K_3Fe(CN)_6$ (0.05 mol/L) (all chemicals were technical grade and purchased from Boom, Meppel, The Netherlands). This electrolyte is pumped through the anode and cathode compartment at a rate of 60 mL/min. Used were Ru-Ir mixed metal oxide electrodes, obtained from Magneto (Magneto Special Anodes b.v., The Netherlands).

3.1.3. Set up

The tests with the R1.0-stacks were done in a recirculating system with centrifugal pumps. Flows in the stack with 50 cells were about 2 L/min for both types of water. For the experiment with the F0.2-stacks, peristaltic pumps were used. The stack with 50 cells was fed with 700 mL/min. In both cases, smaller stacks were fed with proportional lower flow rates. This lower flow rate in the F0.2 stems from a higher hydrodynamic resistance of the thinner spacers. The temperature was about 24–25 °C for all experiments. The used salt concentrations were 1 and 30 g/L of NaCl.

3.2. Power measurements

On the R1.0-stacks, the voltage was measured between the work and the counter electrode. The F0.2-stacks were fitted with two little platinum electrodes in the middle of the work and the counter electrode. Stack potentials were measured in the anolyte and catholyte between these reference Pt electrodes whereas the current was applied to the working and counter electrode.

Measurements were done with an Ivium potentiostat (Ivium Technologies, Eindhoven, The Netherlands) in the galvanostatic mode. From the measured $U(I)$-curves the power was calculated as the maximum of the product from U and I and the resistance was calculated as the slope of the $U(I)$ curve at the maximum power.

3.3. Calculation of the resistances r, R and ρ in a single cell

For comparing the electric characteristics of a R1.0-stack with a F0.2-stack it is necessary to know the resistances r, R and ρ. These parameters, which are typical cell properties, were calculated as well as possible. Afterwards the internal resistance r was experimentally determined in small stacks with 0, 1, . . ., 5 cells.

3.3.1. The internal resistance r

The internal resistance can be calculated from the membrane specifications at 0.5 mol/L NaCl (near to 30 g/L), given by the

Table 1
Resistance (Ω) of one cell of 0.01 m^2 for various cell designs

	Spacer: 1.0 mm		Spacer: 0.2 mm		Spacer: 0.1 mm	
	Ralex	Fumasep	Ralex	Fumasep	Ralex	Fumasep
AEM	0.080	0.008	0.080	0.008	0.080	0.008
CEM	0.080	0.008	0.080	0.008	0.080	0.008
Sea (30 gNaCl/L)	0.026	0.026	0.005	0.005	0.003	0.003
River (1 g NaCl/L)	0.629	0.629	0.126	0.126	0.063	0.063
Total	0.815	0.671	0.291	0.147	0.225	0.081
Ratio Ralex/Fumasep	1.21		1.98		2.77	

membrane supplier. The ionic resistance for Ralex membranes (8 Ω cm^2) is 10 times higher than the Fumasep membranes (0.8 Ω cm^2). It is assumed that the area resistance is independent of the salinity. A void factor $f_v = 0.80$ is used for the resistance of the water compartments.

Table 1 shows that the stack resistance is only reduced significantly if low resistance membranes are combined with thin spacers.

3.3.2. The feed and drain channel resistance R

As explained earlier, only the salt water channels are taken in account. The channel resistance R is calculated from the dimensions of the cylindrical bore through the cell and the conductivity of the salt water. In fact on the place where the channel crosses a spacer, the width of the channel increases. If we assign a zero resistance to this passage, the channel resistance is somewhat lower than the formerly calculated value. A good approximation is the average of the two mentioned values. Because R stands for two parallel resistances (feed and drain) in the model, this resistance value should be halved. The resistances calculated in this manner are 3.9 Ω for the R1.0-stack and 0.81 Ω for the F0.2-stack.

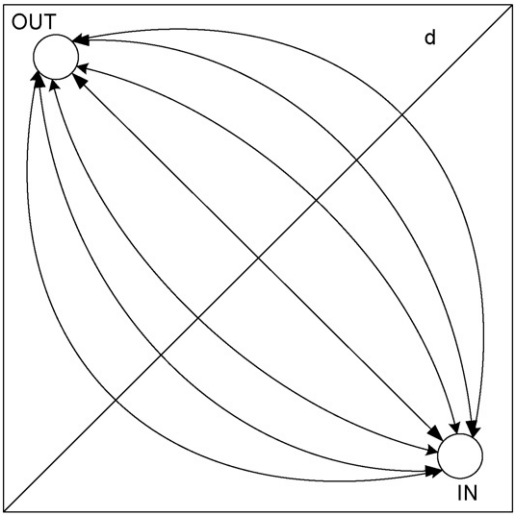

Fig. 6. The lateral ionic shortcut currents in a seawater compartment. These currents originate from each point in the compartment and are directed by the electrical field to the inlet and outlet holes.

3.3.3. The lateral spacer resistance ρ

Fig. 6 shows the configuration of the salt water compartment with the inlet and outlet in two opposite corners. From each point in the compartment there is a useful current perpendicular to the membranes through the cell and small lateral ionic shortcut currents in the direction of the feed and drain channels. In principle this is a three-dimensional potential flow problem. However, the described equivalent circuit model asks for only one single value of a spacer resistance (ρ). To estimate ρ, some approximations are applied. First, the resistance between inlet and outlet is calculated with a two-dimensional potential flow model. The second step is the assumption that the current source lies on the diagonal d. In that case the resistance from the diagonal to the corner is half the corner-to-corner resistance. The results of the calculations are: $\rho = 142$ Ω for the R1.0-stack and $\rho = 710$ Ω for the F0.2-stack.

3.3.4. All calculated resistances together

In Table 2 the calculated resistances for R, ρ and r are summarized.

3.4. Experimental procedure

The equivalent circuit model was calibrated and validated (Fig. 7). The calibration was performed successively with a stack of 5, 4,. . ., 0 cells. In the case of a small number of cells (N), the ionic shortcut currents through the spacers (ρ) and the channels (R) are negligible. Therefore, the calculation of E and r is rather straightforward. For each stack, the OCV was measured and the internal resistance (R_i) at maximal power was measured. From the slope of the regression lines of OCV versus N and R_i versus N, the EMF (E) and the cell resistance (r) were determined.

For the validation, experiments were done with larger stacks with 50, 40, . . ., 10 cells. Here the OCV and the maximal power were measured. These values were compared with the forecasted values calculated with the equivalent circuit model. In this model

Table 2
Calculated resistances

	R1.0	F0.2
r Cell (Ω)	0.815	0.147
R Channel (Ω)	3.9	0.81
ρ Spacer (Ω)	142	710

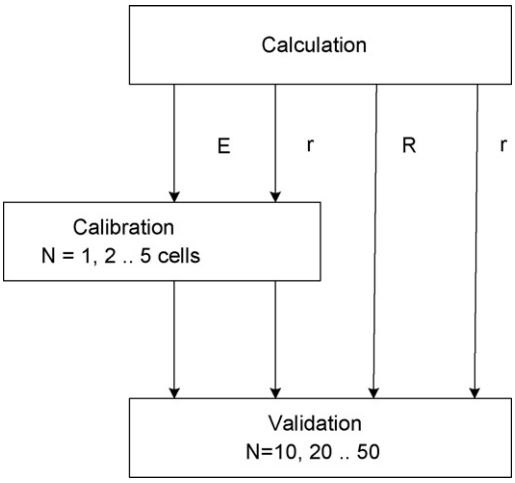

Fig. 7. The validation procedure of the equivalent current model.

the EMF (E) and the cell resistance (r) from the calibration procedure were used together with the channel resistance (R) and the lateral spacer resistance (ρ) from the calculations in the previous Sections 3.3.2 and 3.3.3.

The procedure is performed with the two types of stacks. In each case the series was started with the complete stack of 50 cells and ended with the small stacks.

4. Results and discussion

4.1. Calibration: measurement of r and E

(a) The R1.0-stack

The resistance is measured in a RED stack with 4, 3, 2, 1 and 0 cells (Fig. 8A). In the case of 0 cells, only one cation exchange membrane (CEM) is placed between the electrode compartments. As seen in Table 3, at $N = 0$, the resistance of the electrode system together with one CEM is 2.62 Ω and the resistance of one RED cell is 1.54 Ω. The EMF of a single cell (E) was obtained from the slope of the OVC regression line (Fig. 8C).

(b) The F0.2-stack

In Fig. 8B, the result is shown for stacks with 5, 4, . . ., 1 cells. Because the voltage is measured between the platinum electrodes, the intercept of the R_i-axis is equivalent to the resistance of only one CEM. Fig. 8D shows the OCV regression line from which the E value is calculated. All regression results are listed in Table 3.

The EMF's are lower than the calculated value of 0.158 V for a cell with ideal membranes. The ratio between measured and calculated values can be interpreted as an average permselectivity α of the CEM and AEM. The ratios calculated from these values are $\alpha = 0.88$ for the Ralex membranes in the R1.0-stacks and $\alpha = 0.94$ for the Fumasep membranes in the F0.2-stacks.

Table 3
Measured internal resistances (R_i) and OCV's as a function of the number of cells (N)

R1.0	F0.2
$R_i = 1.54\ N + 2.62$, $R^2 = 0.9830$	$R_i = 0.28\ N + 0.12$, $R^2 = 0.9977$
OCV = $0.139\ N + 0.003$, $R^2 = 0.9998$	OCV = $0.148\ N + 0.001$, $R^2 = 0.9999$

Table 4
Used input parameters in the model

	Source	R1.0	F0.2
E (V)	Experimental ($N = 1, 2, \ldots, 5$)	0.139	0.148
r (Ω)		1.54	0.281
R (Ω)	Calculated	3.9	0.81
ρ (Ω)		142	710

In the R1.0-stack with 1 mm spacers the measured value of the cell resistance is almost twice the calculated value with Eq. (3) (measured 1.54 Ω; calculated 0.815 Ω). The same holds for the F0.2-stack (measured: 0.28 Ω; calculated 0.147 Ω). For these differences between the calculated and measured values some reasons are suggested:

- The membrane specifications hold for membranes immersed in 0.5 M NaCl solution. This value is near the used seawater concentration of 30 g/L. But the membranes in the stack are immersed between solutions of 1 and 30 g/L. A lower salt content increases the resistance of the membranes. A model is suggested by Zabolotsky and Nikonenko [17] in which homogeneities are present on microscale. The included water phase and the solid membrane phase are described as a resistor network. The salt concentration in the water part of this network is dependent of the external concentration, causing an overall concentration dependent resistance of the membrane.
- The ionic current through the spacer grid is not straightforward, but tortuous.
- Stagnant depletion and enrichment layers can be formed on both sides of the membranes.
- The membranes are covered partly by the spacer material. This is sometimes called the shadow effect.

4.2. Validation of the model

With the two types of stacks, experiments were done with a variable number of cells (N) in the range from 10 to 50. With the described model the stack performance was also calculated. The values of the used parameters are listed in Table 4. Fig. 9 shows the measured open circuit voltage and the power, plotted against the number of cells (N). Each graph shows the measured data (squares), the forecasted values by the equivalent circuit model (the solid line) and the extrapolation of the first two data points (the dashed line). The dashed lines represent an 'ideal stack'. Calculated and measured data are very close together, indicating that the model is valid.

4.3. Implementation of the model

For the used R1.0-stack, currents and dissipated powers are calculated with the equivalent circuit model for a stack containing 4 and 50 cells. The external resistance was adjusted such that

Table 5
Calculated generated external power (P_u) and dissipated power P_{dis} in % in different parts of a R1.0-stack with 4 and 50 cells

	$N=4$	$N=50$
P_u (%)	46.7	31.3
P_{dsi} in r (%)	51.7	61.6
P_{dis} in R (%)	0.1	5.9
P_{dis} in ρ (%)	1.5	1.2
Total (%)	100.0	100.0

a maximal power was achieved. The values used are $\rho = 142\ \Omega$, $R = 3.9$, $r = 1.54\ \Omega$ and $E = 0.150$ V. With the same resistances the calculations are repeated for a stack of 50 cells. Fig. 10A shows all currents in a R1.0-stack with 50 cells as function of the position n in the stack ($1 \leq n \leq N$). In Fig. 10B, the cell voltage is plotted for the same stack. The distribution of the dissipated power in the different parts of R1.0-stacks with 4 and 50 cells is given in Table 5.

The ionic shortcut currents cause a voltage drop over the individual cells (Fig. 10B). Also here a flattening is seen in the middle of the stack. Fig. 10A shows the same flattening effects, discussed already in Section 2.6 for very large stacks. Only the first and final ten lateral spacer currents (j) appear to be significant. Assuming a number of 10 lateral spacer resistances of 142 Ω at the beginning, the result is a connection between the main route and the bypass of 14.2 Ω. This value is low compared to the resistance of the bypass channel ($50 \cdot 3.9 = 145\ \Omega$).

Table 6
The efficiency at stacks with 50 cells and with a very large number of cells

	R1.0	F0.2
Test value $N \cdot R/\rho (N=50)$	1.6	0.06
Efficiency at $N=50$ (%)	77	94
Efficiency at $N \rightarrow \infty$ (%)	72	74

It is evident that longer stacks have a more serious loss of power by shortcut currents but they do not exceed the limit values of very large stacks. If the saturation of the shortcut current is not reached already, an improvement of the efficiency can be achieved by an increase of both R/r as ρ/r.

The test value ($N \cdot R/\rho$) and the efficiency at $N = 50$ and at very large values of N for both studied stacks are summarized in Table 6. With the used test ($N \cdot R/\rho = 1.6$), the R1.0-stack with 50 cells is already 'very large' and operates near the efficiency limit. In this case of very large cells an improvement can be achieved only by increasing the ratio R/r. A higher ρ/r ratio has less effect on the efficiency.

A stack consists of an electrode system and N cells. It is shown above that the shortcut currents are minimal at low N. The electrochemical parameters of the used electrode system

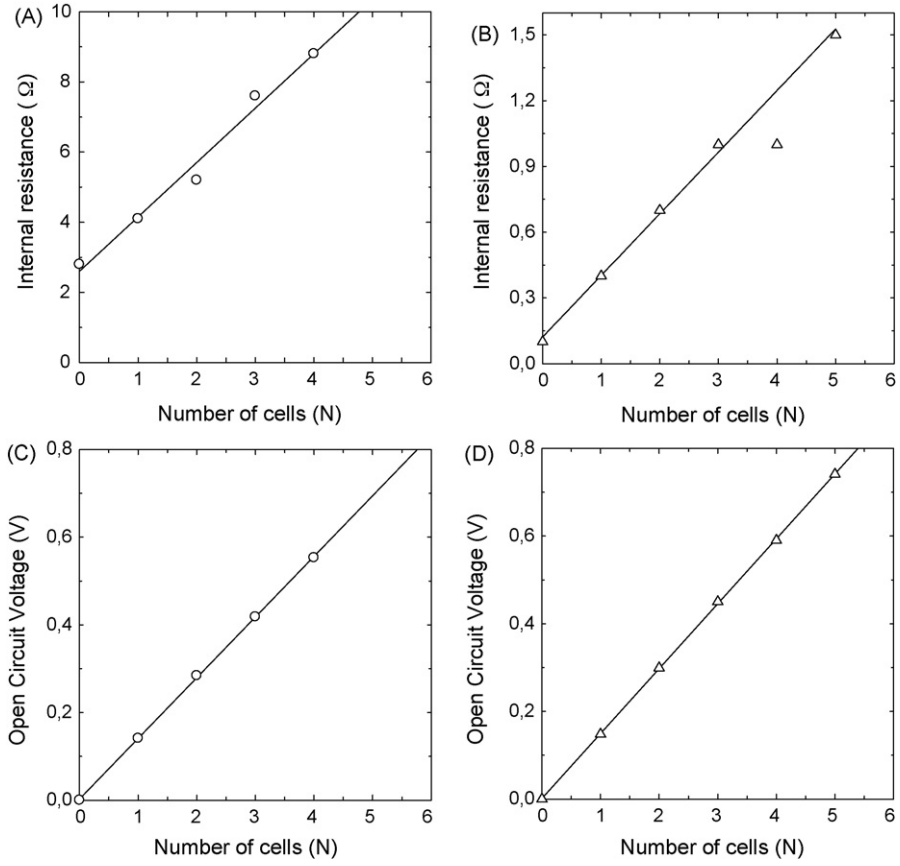

Fig. 8. (A and B) Measured stack resistances. (A) Resistance of R1.0-stacks measured between the working electrode and the counter electrode. (B) Resistance of the F0.2-stacks measured between two platinum reference electrodes. For the calculation of the regression line, the point at $N = 4$ is considered as an outlier and omitted. (C and D) Measured open circuit voltages. (C) OCV of a R1.0-stack. (D) OCV of a F0.2-stack.

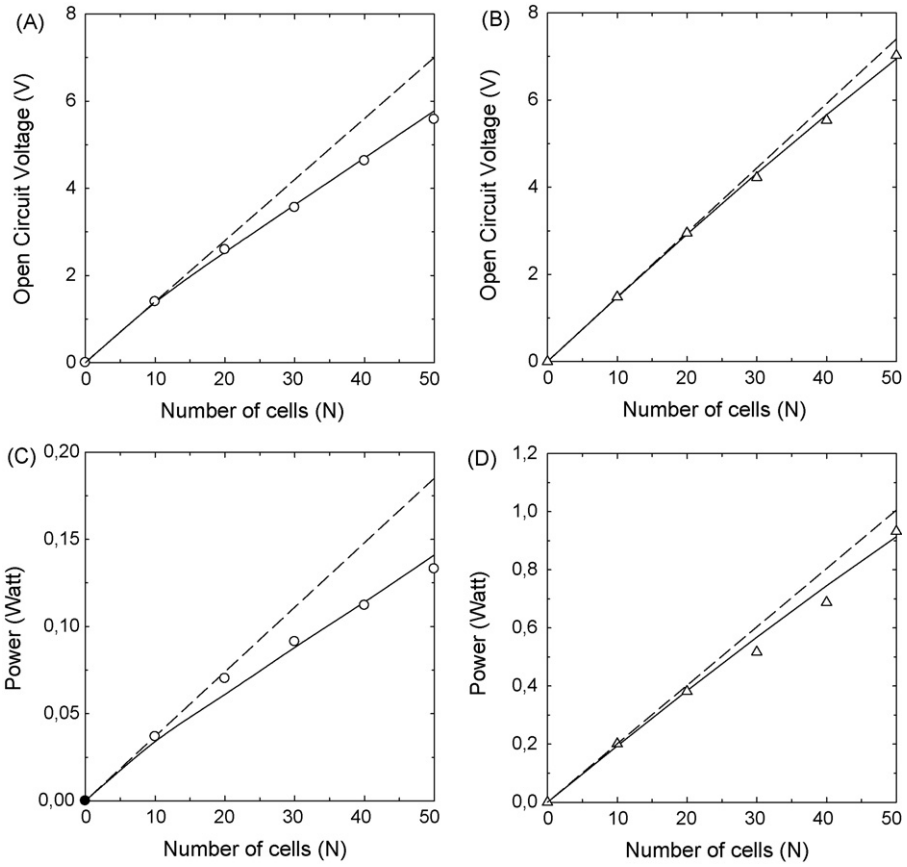

Fig. 9. (A and B) Measured and calculated open circuit voltage (A: R1.0-stacks; B: F0.2-stacks). The solid lines represent the calculated values, the symbols represent the measured values, and the dashed line is the extrapolation of the first two measured data points. (C and D) Equivalent graphs for the dissipated power (C: R1.0-stacks; D: F0.2-stacks).

are important for calculation of the optimal number of cells. Moreover, at real (economically operating) RED installations the price of the electrode system should be taken into account in the optimization as well, resulting in a value of N that is as large as possible, and that is only restricted by the available space. Table 6 shows that for such large stacks, the efficiency reaches a limiting value.

4.4. The validated model expressed in one plot

The equivalent circuit model has been used to calculate various stack designs. The maximum power is calculated for 75 combinations of the channel resistance R (1, 3 and 10 Ω), the spacer resistance ρ (1, 3, 10, 100 and 300 Ω) and the number of cells n (2, 3, 10, 30 and 50). The following assumptions were

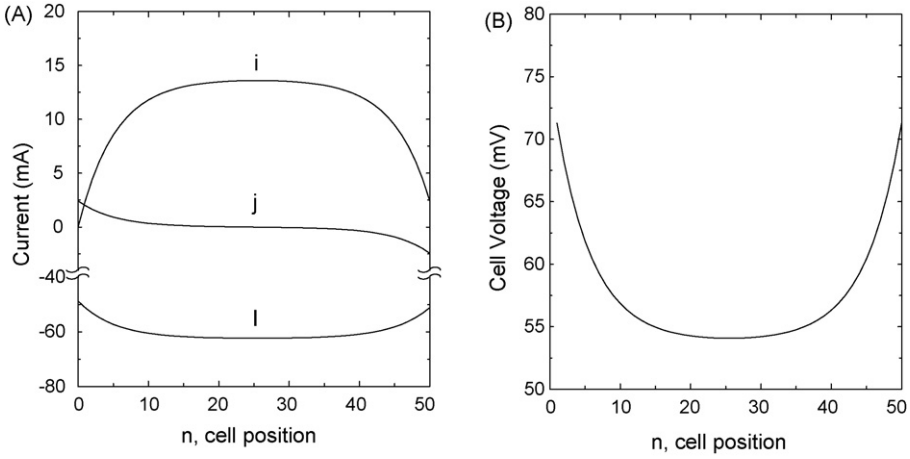

Fig. 10. (A) Calculated currents (j, i and I) in a R1.0-stack with 50 cells through the different resistances (ρ, R and r). The cell position n indicates the location in the stack. (B) The calculated voltage over the individual cells in a R1.0-stack.

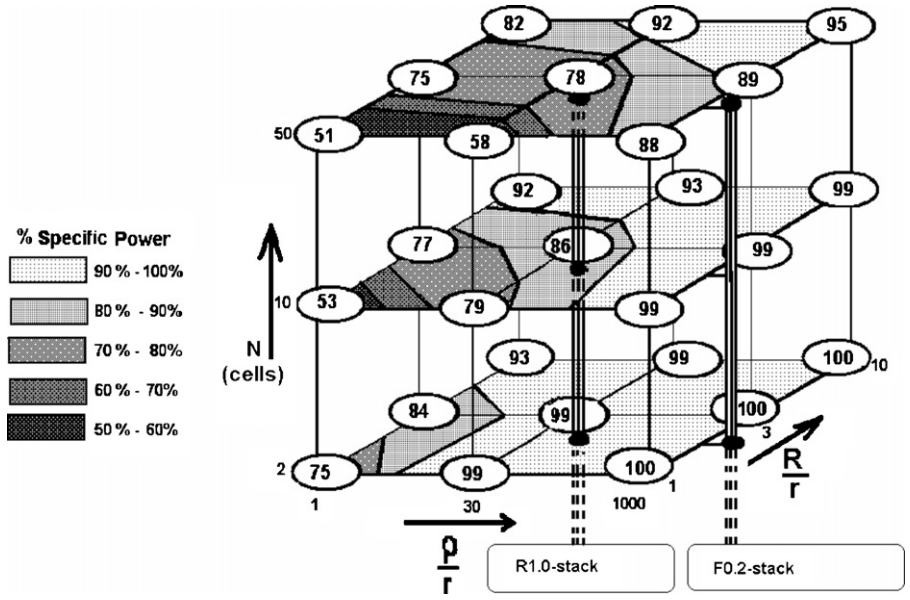

Fig. 11. Power ratio (the values in the circles in %) as function of N, R/r and ρ/r. The lines between the different colors are the 90% borders, the 80% borders and so on.

used for the calculation: $E = 0.15$ V and $r = 1\ \Omega$ for a single cell. The ideal power (P_{ideal}) is also calculated for each number of cells N by applying large values for ρ and R in the model. Power is expressed as the power ratio ($P_R = P/P_{ideal}$).

In fact, by taking one of the resistances unity ($r = 1$), the values of ρ and R can be considered as the relations ρ/r and R/r. So the power ratio is a function of these two relative resistances and of the number of cells N:

$$P_R = f\left(\frac{\rho}{r}, \frac{R}{r}, N\right) \tag{14}$$

The three variables form a three-dimensional space and at some points in this space the P_R-values (in %) are given in circles to give a kind of a four-dimensional plot (Fig. 11).

The data for the described two stacks: the R1.0-stack ($R/r = 2.5$; $\rho/r = 94$) and the F0.2-stack ($R/r = 2.9$; $\rho/r = 2580$) is given in the plot as well. The F0.2-stack operates at 94% efficiency with 50 cells. Expansion of the stack to 250 cells will cause an estimated efficiency drop to about 80% going to a limit of 74% for very large stacks. A 50-cell R1.0-stack operates at an efficiency of 77% near to the limit of 72% for large stacks.

From this plot in it follows that at stacks with a medium number of cells, R/r and ρ/r should be as high as possible. This can be achieved by: (a) increasing R by narrowing the channels, (b) increasing ρ by taking thinner spacers (especially in the sea water compartment) (c) decreasing r by using low resistive membranes and thin spacers (especially the river water compartment). The possibilities to maximize R are limited because the hydro dynamical resistance in the channels increases with narrowing of the channels. In a cylindrical tube with radius r, the electrical resistance is proportional with r^2 whereas the fluid resistance is related to r^4, assuming Poiseuille flow dynamics. A benefit with a factor x in the electrical resistance is paid for with a factor x^2 in the fluid resistance. Increasing ρ influences the relative power only marginal in large stacks as explained in the previous section. However, decreasing r seems to be very opportune as it causes not only a higher efficiency but also an expansion of the specific power.

In addition the theory described in Section 2.6 for very large stacks, improvements can be obtained by optimizing R/r. Decreasing r by minimization of both compartments and both membrane thicknesses results in an equal decrease of R resulting in an unaffected ratio R/r. However, Table 1 shows the river water compartment is the bottleneck in the resistance. In very large stacks reduction ρ/r is not opportune, so there is no need for thinning the sea water compartments. However, with given membrane and river water compartment dimensions, decrease of only the thicknesses of the sea water compartment results in (i) a higher R/r ratio and therefore in a higher efficiency (ii) a lower r, so a higher specific power of the stack.

5. Conclusions

In this work, a model for the ionic shortcut currents in a reverse electrodialysis stack is presented. The model is calibrated and validated on two different stacks. Our main findings are:

- Measured cell resistances are about a factor two higher than calculated. This deviation might stem from (i) a strong concentration dependent behavior of the membranes, (ii) a restricted ionic transport in the spacers (iii) a stagnant depletion and enrichment layers on both sides of the membranes, (iv) a shadow effect from the spacer on the membranes.
- It is possible to describe the ionic shortcut loss with only three parameters: (i) the number of cells N, (ii) the channel resistance in proportion to the cell resistance R/r, (iii) the lateral spacer resistance in proportion to the cell resistance ρ/r.

- The equivalent circuit model was calibrated and validated with two different kinds of stacks. One type was built with Ralex membranes and 1 mm spacers, the other stack contained Fumasep membranes and spacers of 0.2 mm. Calibration was done with small stacks of 1, 2 to 5 cells and validation with large stacks of 10, 20 to 50 cells. The calculated and measured values of power and OCV's were in very good agreement.
- With the used Fumasep stack with 0.2 mm spacers, the loss caused by ionic shortcut currents is 6% for a stack with 50 cells, showing that the ionic shortcut currents are manageable.
- In very large stacks, increase of the ratio between the channel resistance and the cell resistance (R/r) is the most efficient measure for reduction of the ionic shortcut current loss.

Acknowledgements

The Noordelijke Hogeschool Leeuwarden has facilitated this research by detaching the first author. Also the Senter Novem organization is gratefully acknowledged for their grant. We thank all members of the energy theme from Wetsus for their support and fruitful discussions and especially the participating companies Nuon, Magneto, Triqua, Landustrie, Frisia Zout and the Waterlab Noord for their support.

Nomenclature

a	activity
a^+	activity of the sodium ion
a^-	activity of the chloride ion
A_{cell}	cell area (m^2)
E	electromotive force of one cell (V)
Eff	efficiency of a RED battery
f_v	void factor f_v
F	Faraday constant (96485 C/mol)
i	the current through the feed and drain channels (A)
I	electrical current perpendicular on the membranes (A)
j	the lateral current leakage along the membrane surface (A)
n	position of a special cell in a stack ($1 \leq n \leq N$)
N	number of cells in a stack
OCV	open circuit voltage (V)
P_{dis}	dissipated power (W)
P_{ideal}	ideal power (W)
P_{max}	maximum external power
P_R	power ratio
P_{spec}	specific power (W/m^2)
P_u	external power (W)
r	cell resistance (Ω)
R	gas constant (8.31432 J mol^{-1} K^{-1}), in Eq. (1)
R	channel resistance of one cell in a stack (Ω)
R^2	determination coefficient
R_{AEM}	cation exchange membrane resistance (Ω)
R_{CEM}	cation exchange membrane resistance (Ω)
R_{comp}	compartment resistance (Ω)
R_{el}	electrode system resistance (Ω)
R_i	internal resistance (Ω)
R_{rel}	relative resistance
R_{river}	river water compartment resistance (Ω)
R_s	total bypass resistance (Ω)
R_{sea}	sea water compartment resistance (Ω)
R_u	external resistance (Ω)
T	temperature (K)
U	the potential at the centre of the membrane (V)
V	the potential in the feed and drain channel (V)
V_t	terminal voltage (V)
z	valency

Greek symbols

α_{CEM}	permselectivity of the cation exchange membrane
α_{AEM}	permselectivity of the anion exchange membrane
δ	compartment thickness (m)
σ	specific conductivity (S/m)
ρ	lateral spacer resistance (Ω)

Abbreviations

AEM	anion exchange membrane
CEM	cation exchange membrane
ED	electrodialysis
EMF	electromotive force (V)
RED	reverse electrodialysis
R1.0	stack with Ralex membranes and 1 mm spacers
F0.2	stack with Fumasep membranes and 0.2 mm spacers

Definitions

compartment	space between the membranes
cell	combination of two membranes and two compartments
electrode system	the anode, cathode, electrode rinse and also one terminating membrane
stack	a number of cells with an electrode system

References

[1] J.W. Post, J. Veerman, H.V.M. Hamelers, G.J.W. Euverink, S.J. Metz, K. Nymeijer, C.J.N. Buisman, Salinity-gradient power: evaluation of pressure-retarded osmosis and reverse electrodialysis, J. Membr. Sci. 288 (2007) 218–230.
[2] R.E. Pattle, Improvements relating to electric batteries, Patent GB731729 (1955).
[3] W.G.B. Mandersloot, R.E. Hicks, Leakage currents in electrodialytic desalting and brine production, Desalination 1 (1966) 178–194.
[4] R. Yamane, M. Ichikawa, Y. Mizutani, Y. Onoue, Concentrated brine production from sea water by electrodialysis using ion exchange membranes, Ind. Eng. Chem. Process Des. Dev. 8 (1969) 159–165.
[5] B.R. Bligh, Reverse electrodialysis, Patent GB2197116A (1988).
[6] T. Wen, G.S. Solt, Y.F. Sun, Spirally wound electrodialysis (SpED) modules, Desalination 101 (1995) 79–91.
[7] T. Wen, G.S. Solt, Y.F. Sun, Modelling the cross flow spirally wound electrodialysis (SED) process, Desalination 103 (1995) 165–176.

[8] T. Wen, G.S. Solt, D.W. Gao, Electrical resistance and coulomb efficiency of electrodialysis (ED) apparatus in polarization, J. Membr. Sci. 114 (1996) 255–262.
[9] A.T. Kuhn, J.S. Booth, Electrical leakage currents in bipolar cell stacks, J. Appl. Electrochem. 10 (1980) 233–237.
[10] J. Pretz, E. Staude, Reverse electrodialysis (RED) with bipolar membranes, an energy storage system, Ber. Bunsen-Ges. Chem. 102 (1988) 676–685.
[11] I. Rubinstein, J. Pretz, E. Staude, Open voltage in a reverse electrodialysis cell, Phys. Chem. Chem. Phys. 3 (2001) 1666–1667.
[12] J.N. Weinstein, F.B. Leitz, Electric power from differences in salinity: the dialitic battery, Science 191 (1976) 557–559.
[13] B.H. Clampitt, F.E. Kiviat, Energy recovery from saline water by means of electrochemical cells, Science 194 (1976) 719–720.
[14] J. Jagur-Grodzinski, R. Kramer, Novel Process for direct conversion of free energy of mixing into electric power, Ind. Eng. Chem. Process Des. Dev. 25 (1986) 443–449.
[15] R.E. Lacey, Energy by reverse electrodialysis, Ocean Eng. 7 (1980) 1–47.
[16] D.C. Harris, Quantitative Chemical Analysis, sixth ed., W. H. Freeman & Company, 2003.
[17] V.I. Zabolotsky, V.V. Nikonenko, Effect of structural membrane inhomogeneity on transport properties, J. Membr. Sci. 79 (1993) 181–198.